Cell, Vol. 120, 223–235, January 28, 2005, Copyright ©2005 by Elsevier Inc. DOI 10.1016/j.cell.2004.11.051

Shisa Promotes Head Formation through the Inhibition of Receptor Protein Maturation for the Caudalizing Factors, Wnt and FGF

Akihito Yamamoto,[1,*] Takashi Nagano,[1] Shoko Takehara,[1] Masahiko Hibi,[2] and Shinichi Aizawa[1,*]
[1]Laboratory for Vertebrate Body Plan
[2]Laboratory for Vertebrate Axis Formation
RIKEN Center for Developmental Biology
2-2-3 Minatojima Minami, Chuou-ku
Kobe 650-0047
Japan

Summary

Head formation requires simultaneous inhibition of multiple caudalizing signals during early vertebrate embryogenesis. We identified a novel antagonist against Wnt and FGF signaling for head formation, Shisa, which functions cell autonomously in the endoplasmic reticulum (ER). Shisa is specifically expressed in the prospective head ectoderm and the Spemann organizer of *Xenopus* gastrulae. Overexpression of Shisa inhibited both Wnt and FGF signaling in *Xenopus* embryos and in a cell line. Loss of Shisa function sensitized the neuroectoderm to Wnt signaling and suppressed head formation during gastrulation. Shisa physically interacted with immature forms of the Wnt receptor Frizzled and the FGF receptor within the ER and inhibited their posttranslational maturation and trafficking to the cell surface. Taken together, these findings indicate that Shisa is a novel molecule that controls head formation by regulating the establishment of the receptors for caudalizing factors.

Introduction

During early vertebrate embryogenesis, the Spemann organizer plays an important role in dorso-ventral (DV) and anterior-posterior (AP) axis formation (Harland and Gerhart, 1997; De Robertis et al., 2000). Many of the secreted molecules emanating from the Spemann organizer function as inhibitors for ventralizing and/or caudalizing factors (referred to as "caudalizing factors"). These include the BMP inhibitors Noggin, Chordin, and Follistatin; the Wnt inhibitors Dickkopf-1 (Dkk-1) and secreted Frizzled-related protein (Frzb-1); the Nodal inhibitors Lefty/Antivin; and the multipotent inhibitor protein, Cerberus (Smith and Harland, 1992; Sasai et al., 1994; Bouwmeester et al., 1996; Meno et al., 1996; Fainsod et al., 1997; Leyns et al., 1997; Wang et al., 1997; Glinka et al., 1998; Thisse and Thisse, 1999). These factors are known to interact directly with caudalizing factors or their receptors and thereby to control the formation of the anterior neuroectoderm in a non-cell-autonomous manner. These factors function cooperatively and partially redundantly with each other, and it has been proposed that combinatorial or simultaneous inhibition of the caudalizing signals is required for head induction (Niehrs, 1999). Inhibition of BMP and Wnt signaling (Glinka et al., 1997), or BMP, Wnt, and Nodal signaling by Cerberus (Piccolo et al., 1999), leads to secondary head induction in *Xenopus* embryos. However, cell-autonomous regulatory mechanisms that may attenuate the caudalizing signals within the anterior neuroectoderm or the organizer, and possible involvement of other caudalizing signals, remain largely unknown. Fibroblast growth factor (FGF) was initially proposed to be a caudalizing factor, as the activation and inhibition of FGF signaling lead, respectively, to reduction and expansion of the anterior neuroectoderm in *Xenopus* embryos (Cox and Hemmati-Brivanlou, 1995; Lamb and Harland, 1995; Monsoro-Burq et al., 2003). However, molecule(s) that directly inhibit FGF signaling and promote head formation during gastrulation have not been identified.

Wnt and FGF constitute families of pleiotropic factors that function in cell growth, differentiation, and body/tissue patterning. Wnts bind to cell surface receptor complexes composed of the seven-pass transmembrane protein Frizzled and the LDL receptor-related protein LRP5/6. In the canonical Wnt signaling pathway, this receptor complex transduces the signal to the cytoplasmic protein Dishevelled (Dsh), which suppresses the activity of a protein kinase GSK3, stabilizes β-catenin, and activates downstream targets (Cadigan and Nusse, 1997; Moon et al., 2002; http://www.stanford.edu/~rnusse/wntwindow.html). FGF binds to the receptor tyrosine kinase FGF receptor (FGFR1-4) and induces its dimerization and transphosphorylation of the FGFR. Subsequently, the small GTPase Ras transmits the FGFR signal and activates the protein kinase cascade Raf-MEK1/2-ERK1/2, which phosphorylates and activates various transcription factors (Hunter, 1998).

To establish these signaling pathways, growth factors and their cognate receptors are generated through the endoplasmic reticulum (ER), where they are subjected to glycosylation and folding. Correctly glycosylated and folded membrane proteins are transported to the cell surface to perform their functions. Proteins with defects in glycosylation and/or folding are trapped in the ER and subsequently degraded by a "quality control (QC) system" (Tsai et al., 2002; Ellgaard and Helenius, 2003; Trombetta and Parodi, 2003). A few proteins are reported to function in the maturation or intracellular trafficking of particular growth factors and growth factor receptors in the ER. Porcupine (Por)/Mom-1 is required for N-glycosylation and transportation of Wnt ligand (van den Heuvel et al., 1993; Kadowaki et al., 1996; Thorpe et al., 1997), while Boca/Mesd functions as a chaperone for the Wnt co-receptor LRP5/6 (Culi and Mann, 2003; Hsieh et al., 2003). Both Por/Mom-1 and Boca/Mesd function in the maturation or translocation of their target proteins and are specifically required for Wnt signaling. However, the regulatory mechanisms that control the maturation or transport of ligands or receptors in the Wnt and other signaling pathways remain largely unknown.

Here we report the isolation of Shisa, a novel molecule

*Correspondence: akihito@cdb.riken.jp (A.Y.), saizawa@cdb.riken.jp (S.A.)

involved in head formation. Shisa interacts with immature forms of the Wnt receptor Frizzled and the FGF receptor within the ER, and suppresses their maturation and trafficking to the cell surface. Experimentally induced loss of Shisa function in *Xenopus* embryos revealed that Shisa is an essential factor for head formation, providing a novel cell-autonomous mechanism by which the anterior head territory avoids respecification by caudalizing signals.

Results

Shisa Is a Novel Molecule Involved in Head Formation

To identify novel genes involved in vertebrate head formation, we performed a cDNA subtraction screening and isolated genes expressed in the *Xenopus* anterior-dorsal endomesoderm at the mid-gastrula period (see Experimental Procedures). One of the genes isolated showed specific expression in the prospective head ectoderm and the organizer (see below) and was named *shisa* (after a form of sculpture, common to southern Japan, with a large head similar to the Egyptian sphinx). The open reading frame of *shisa* consists of 269 amino acids (GenBank accession number AY579372). Database searches revealed homologs in human, mouse, and zebrafish (Supplemental Figure S1 at http://www.cell.com/cgi/content/full/120/2/223/DC1/). Shisa contains a signal peptide and two cysteine-rich domains in the amino-terminal half (Cy1 and Cy2 in Figure 1A). There is a hydrophobic region at the amino-terminal to the Cy2 region (Supplemental Figure S1) that is potentially a transmembrane domain. While the sequence of the amino half was well conserved over the species, that of carboxy half was divergent (Supplemental Figure S1); no known protein motifs or conserved amino acid sequences were observed. Shisa was found to be secreted from HEK 293T cells (Figure 1B) and was detected in the ER of *Xenopus* blastomeres as well as HEK 293T cells, where calreticulin was also detected (Figures 1C–1D″).

Expression of Shisa in Early *Xenopus* Development

Northern blotting detected a maternal and zygotic 2.5 kb *shisa* transcript (Figure 1E). *shisa* expression increased during gastrulation and decreased during early neurulation. Whole-mount in situ hybridization revealed that the maternal *shisa* transcript was detected in the entire animal hemisphere (data not shown). Zygotic *shisa* expression was initiated at the onset of gastrulation and was detected in the deep endomesoderm of the upper dorsal lip, the Spemann organizer (Figure 1F). With the progress of gastrulation, *shisa* expression occurred in the anterior neuroectoderm; it was first detected in the deep layer of neuroectoderm and after the mid-gastrulation it was also detected in the superficial layer (Figures 1G, 1H, and 1J–1L). The expression in endomesoderm concomitantly became restricted to the future prechordal plate territory (Figure 1G). At the mid-neurula stage, the ectodermal expression declined (Figure 1I), while that in the prechordal plate persisted until the late-neurula stage (data not shown).

Shisa Affects Anterior-Posterior Axis Formation

To examine the function of Shisa, we injected *shisa* RNA into the animal side of each blastomere in 4-cell stage *Xenopus* embryos. A low-dose injection resulted in embryos with enlarged cement glands and anterior head structures (Figure 2A). A single dorsal injection induced expansion of *otx2* expression, which marks prospective fore- and midbrain (Figure 2B), indicating that Shisa promotes head formation. A high-dose injection suppressed the formation of trunk and tail, while it enlarged anterior structures (Figure 2C). A single injection into the ventral marginal zone reduced *Xbra* expression at the mid-gastrula, indicating that Shisa inhibits mesoderm induction (Figure 2D). We next examined the neuralizing activity of Shisa in the animal cap assay, which is also one of the most sensitive assays for BMP signaling inhibition. Animal cap explants from 200 pg *shisa* RNA-injected embryos did not express the neural markers *NCAM* and *N-tubulin* (data not shown), indicating that Shisa has little or no neuralizing activity and is not an effective inhibitor of BMP signaling. Injection of *shisa* RNA into the ventral marginal zone did not induce secondary axes (data not shown), but coinjection with RNA for a dominant-negative BMP receptor (*tBR*) induced secondary heads with an enlarged cement gland and two eyes (Figures 2F and 2G). These data indicate that Shisa is an anteriorizing, but not a dorsalizing or neuralizing, factor in *Xenopus* embryos.

Shisa Antagonizes Wnt and FGF Signaling

The induction of secondary heads is also observed in embryos that receive a ventral coinjection of both BMP and Wnt inhibitors (Glinka et al., 1997). The reduction of trunk and tail mesoderm, and the suppression of the *Xbra* expression, are seen in embryos expressing a dominant-negative FGF receptor (dnFGFR) (Amaya et al., 1991). These previous reports, together with the phenotypes of Shisa misexpression, suggest that Shisa is an inhibitor of both Wnt and FGF signaling. To address this issue, we examined the effects of Shisa on Wnt and FGF signaling using the animal cap assay. In animal cap explants, *Xwnt8* RNA induced the expression of *Xnr-3*, a direct target of the canonical Wnt pathway (Brannon et al., 1997; McKendry et al., 1997). Coinjection of *shisa* RNA with *Xwnt8* RNA inhibited *Xwnt8*-induced *Xnr-3* expression (Figure 2H, lane 7). However, Shisa did not inhibit *Xnr-3* expression induced by overexpression of Dsh, dominant-negative GSK3β (dnGSK3), or β-catenin (Figure 2H, lanes 8–10), indicating that Shisa inhibits the canonical Wnt pathway upstream of Dsh.

Treatment of animal caps with Activin induced the expression of both *Xbra* and the endodermal marker *mix2,* which is a direct target of Activin (Nodal)/Smad2 signaling (Chen et al., 1996). Cooperation of Activin (Nodal) and FGF signals is required for *Xbra* induction (Cornell and Kimelman, 1994; LaBonne and Whitman, 1994). Shisa inhibited Activin-induced *Xbra* expression but not *mix2* (Figure 2I, lane 4), suggesting that Shisa does not inhibit Activin signaling directly but rather inhibits an event downstream of the Activin (Nodal) signal. The suppression of *Xbra* induction by Shisa was not through inhibition of Wnt signaling, as overexpression of the Wnt inhibitors Dkk-1 and Frzb-1 showed little or

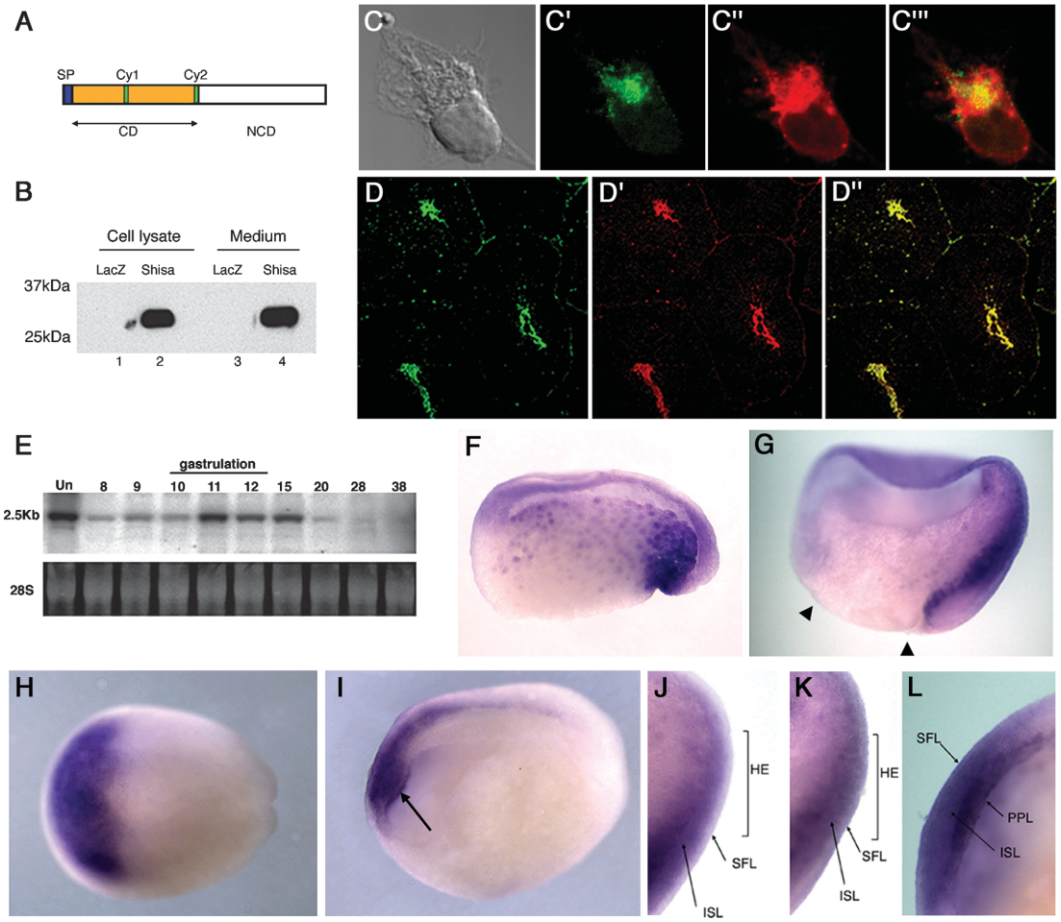

Figure 1. A Novel Protein Shisa and Its mRNA Expression in the Prospective Head Ectoderm and the Organizer of *Xenopus* Gastrulae

(A) Schematic structure of Shisa. SP, N-terminal signal peptide; CD, conserved domain; NCD, nonconserved domain; Cy, cysteine-rich domain.

(B) Secretion of Shisa. Western blotting of conditioned medium or cell lysate from HEK 293T cells transfected with *shisa*-Flag or nuclear-lacZ (control). Molecular weight of secreted Shisa-Flag is 30 kDa.

(C–D″) ER localization of Shisa. HEK 293T cells transfected with *shisa*-Myc (C–C‴) or a cryosection of the late blastula stage embryo radially injected with 50 pg of *shisa*-Flag RNA (D–D″) were stained for Shisa (green) and an ER marker calreticulin (red).

(E) Developmental Northern blotting of *shisa* mRNA. Stages of samples are indicated at top. Hybridization with ^{32}P-labeled *shisa* cDNA is in the middle. Ethidium bromide staining of 28S RNA is at the bottom.

(F–L) Whole-mount in situ hybridization of *shisa* transcripts. (F, G, J, and K) Sagitally sectioned embryos of stage 10.5 (F) and stage 11.5 (G, J, and K). *shisa* expression was found in the Spemann organizer of the early gastrulae. In the prospective head ectoderm at mid-gastrula (stage 11.5, according to the developmental time schedule), 55% of the embryos displayed predominant *shisa* mRNA expression in the internal sensorial layer (ISL in [J]), while 45% had the expression in both superficial layer (SFL) and ISL (K, n = 30). This may be due to slight differences in the developmental stage of each embryo. Arrowheads in (G) indicate blastoderm margin. HE: head ectoderm. (H and L) Dorsal view (H) and sagittally sectioned embryos (L) at the end of gastrulation (stage 13), showing that *shisa* expression covered the anterior head ectoderm (H) of both ISL and SFL (L). PPL: prechordal plate.

(I) Sagittally sectioned neural plate stage (stage 17) showing downregulated *shisa* expression in the head ectoderm and persistence in the prechordal plate (indicated by arrow).

no effect on Activin-induced *Xbra* expression (Figure 2I, Kazanskaya et al., 2000; Semenov et al., 2001). These results suggest that Shisa inhibits FGF signaling directly. Injection of *Xenopus efgf* (*fgf4*) RNA induces *Xbra* (Pownall et al., 1996), and coinjection of increasing amounts of *shisa* RNA suppressed this induction in a dose-dependent manner (Figure 2J). Furthermore, Shisa inhibited bFGF (FGF2)-induced ERK activation in animal cap explants (Figure 2K) but did not inhibit the constitutively active Ras (RasV12)-induced ERK activation (Figure 2L), indicating that Shisa directly inhibits FGF signaling at a level upstream of Ras.

Shisa Is Required for Head Formation during Gastrulation

To investigate the role of Shisa in vivo, we utilized antisense morpholino oligonucleotides for the 5′-untranslated region (UTR) of *shisa* (*shisa*-MO). In embryos that received injections of *shisa*-MO in both blastomeres of the 2-cell stage, the expression of *otx2* was downregulated in the anterior neuroectoderm, but not in the anterior endomesoderm, at the mid-gastrula stage (stage 11.5) (Figure 3C, 72%, n = 90). This phenotype was not observed in embryos that received injections of a control MO (COMO) (Figure 3B, 95%, n = 85) and furthermore

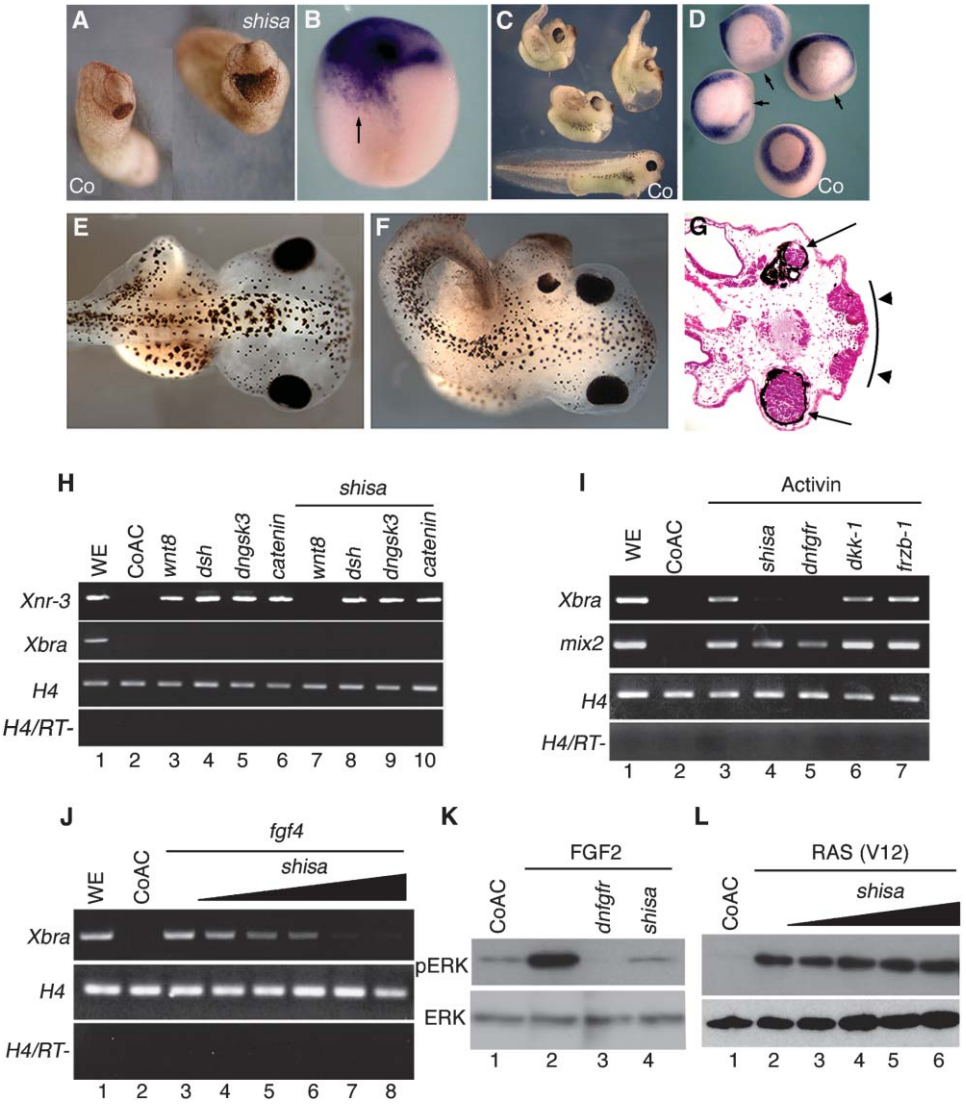

Figure 2. Shisa Promotes Head Formation and Inhibits Wnt and FGF Signaling

(A) Radial injection of *shisa* RNA (50 pg) into the animal side of each blastomere at the 4-cell stage. Note the enlargement of the cement gland and the anterior brain structure (100%, n = 120). Co: uninjected embryo.

(B) A dorsal single blastomere injection of *shisa* RNA (50 pg) induced the ectopic *otx2* expression indicated by arrow (stage 13, 100%, n = 65).

(C) Radial injection of *shisa* RNA (200 pg) impaired trunk formation as well as expanded head structure (95%, n = 80).

(D) A single blastomere injection of *shisa* RNA (200 pg) into the marginal zone. Arrows indicate reduced *Xbra* expression. (100%, n = 45).

(E) Ventral marginal zone injection of *tBR* RNA (250 pg) alone induced secondary trunk structure (55%, n = 82).

(F) Coinjection of *shisa* (50 pg) RNA with *tBR* RNA (250 pg) induced secondary head structures (53%, n = 56).

(G) Histological section of the induced secondary head. Arrows and arrowheads indicate eyes and the enlarged cement gland, respectively.

(H) Shisa inhibited Wnt signaling upstream of Dsh. *Xwnt8* (1 pg), *dsh* (50 pg) *dngsk3* (25 pg), or β-*catenin* (25 pg) RNAs were radially injected either alone or together with *shisa* (50 pg) RNA into each animal blastomere at the 8-cell stage. Animal cap explants (ACs) were isolated at late blastula. RT-: PCR with cDNAs synthesized without reverse transcriptase.

(I) Shisa downregulated *Xbra* expression but not *mix2* in ACs treated with Activin. Lane 1: whole embryo. Lane 2: ACs cultured without Activin. Lanes 3–7: ACs were treated with Activin. RNAs (lane 4, *shisa* 100 pg; lane 5, *dnfgfr* 100 pg; lane 6, *dkk-1* 100 pg; lane 7, *frzb-1* 100 pg per blastomere) were injected as described in (H).

(J) Shisa inhibited FGF4-mediated *Xbra* induction. *fgf4* (0.05 pg per blastomere) RNA was injected either alone or together with *shisa* RNA as described in (H). Lane 1: whole embryo. Lane 2: control ACs. Lane 3: *fgf4* alone. Lanes 4–8: with *shisa* RNA (Lane 4, 12.5 pg; Lane 5, 25 pg; Lane 6, 50 pg; Lane 7, 100 pg; Lane8, 200 pg per blastomere).

(K) Shisa inhibited MAPK activation in ACs treated with FGF2. Lane 1: ACs cultured without FGF. Lanes 2–4: ACs treated with FGF2. RNAs (lane 3, *dnfgfr* 100 pg; lane 4, *shisa* 100 pg per blastomere) were injected as described in (H).

(L) Shisa did not inhibit constitutively activated *ras*-induced MAPK activation. *ras* (V12) RNA (10 pg per blastomere) was injected either alone or together with *shisa* RNA (lane 3, 25 pg; lane 4, 50 pg; lane 5, 100 pg; lane 6, 200 pg per blastomere) as described in (H).

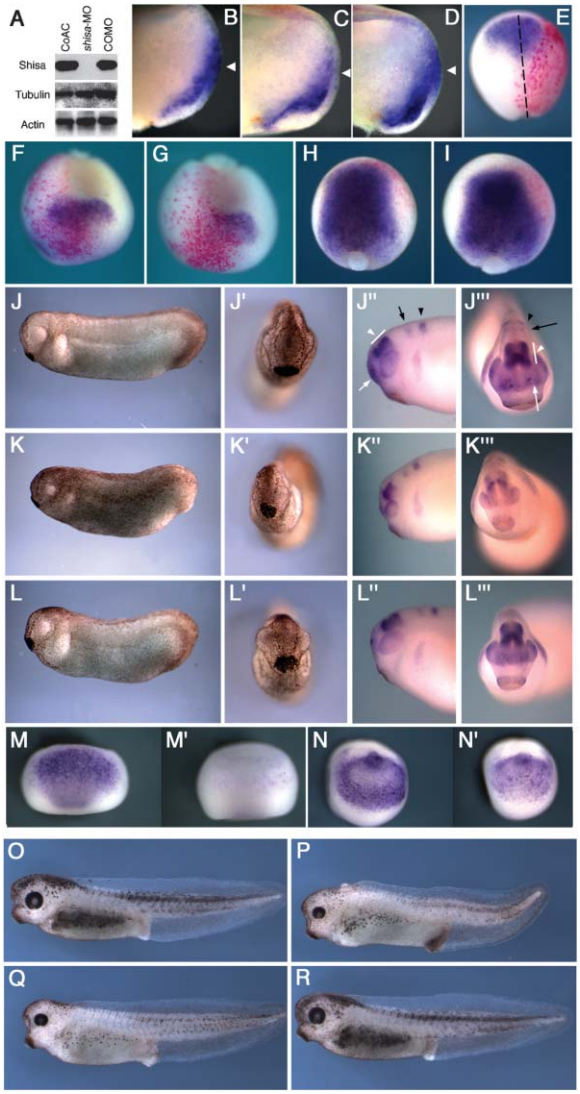

Figure 3. In Vivo Requirement of Shisa in Head Formation

(A) *shisa*-MO (20 ng) specifically inhibited the translation of overexpressed *shisa*-Flag RNA (100 pg) in animal halves explanted at gastrula stage. Tubulin and Actin proteins were served as specificity controls.

(B–D) *shisa*-MO reduced ectodermal *otx2* expression but not that of endomesoderm at mid-gastrula (Stage 11.5). Twenty nanograms of *shisa*-MO (C) or *shisa*-MO in combination with 10 pg of *shisa* RNA (D) was injected into both blastomeres at 2-cell stage. Embryos injected with COMO served as a control (B). White arrowheads indicate the prospective head ectoderm.

(E–I) *shisa*-MO injection reduced expression of *otx2* and *six3* but not that of *sox2* at the end of gastrulation. Twenty nanograms of COMO (F and H) or *shisa*-MO (E, G, and I), together with nuclear lacZ mRNA (200 pg), were injected at the 2-cell stage into a single blastomere. β-galactosidase activity was visualized by red staining. Probes used were *otx2* (E), *six3* (F and G), and *sox2* (H and I).

(J–L‴) *shisa*-MO injections suppressed head formation. Lateral (J, J″, K, K″, L, and L″) and frontal (J′, J‴, K′, K‴, L′, and L‴) views of tail bud stage. Embryos were injected with COMO (J–J‴), *shisa*-MO (K–K‴), or *shisa*-MO with *shisa* RNA (L–L‴) as described in (B)–(D). In situ hybridizations with *otx2* and *krox20* are (J″), (J‴), (K″), (K‴), (L″), and (L‴). White arrows and arrowheads in (J″) and (J‴) indicate *otx2* expression in the telencephalon and midbrain, respectively. Black arrows and arrowheads indicate *krox20* in the rhombomeres 3 and 5, respectively.

was rescued by injection of *shisa* RNA lacking the 5′-flanking region (Figure 3D, 100%, n = 45), indicating that the effects of *shisa*-MO are specific. When *shisa*-MO was coinjected with β-galactosidase RNA into a single blastomere at the 2-cell stage, the expression of *otx2* and the forebrain marker *six3* was reduced in the region that received the injection at the end of gastrulation (Figures 3E–3G, reduction of *otx2*, 75%, n = 68; *six3*, 49%, n = 95). In contrast, expression of the pan-neuroectodermal marker *sox2* was not affected by *shisa*-MO injection (Figure 3I, 100%, n = 55). However, at the early neurula stage, *otx2* expression recovered in the midbrain region in particular, although not in the anterior forebrain or cement gland region (Figure 3N′, 48%, n = 42). At the tail bud stage, injection of *shisa*-MO resulted in embryos exhibiting small heads with small eyes and cement glands (Figures 3K and 3K′, 67%, n = 78). This *shisa*-MO effect was significantly complemented by injection of *shisa* RNA (Figures 3L and 3L′, small heads with small eyes and cement glands, 11%, n = 66). At this stage, *otx2* expression marks the anterior telencephalon, midbrain, and eye field. Rhombomeres 3 and 5 of the hindbrain were stained by *krox20* (Figures 3J″ and 3J‴). *shisa*-MO injection severely reduced the size of *otx2*-positive telencephalon, eye field, and midbrain but did not affect the distance between rhombomeres 3 and 5 (Figures 3K″ and 3K‴, 70%, n = 60). *shisa* RNA coinjected with *shisa*-MO restored telencephalic *otx2* expression and normal eye and midbrain size (Figures 3L″ and 3L‴, reduction of telencephalic *otx2*, 3%, n = 66). At the tadpole stage, *shisa*-MO-injected embryos displayed reductions in the forebrain region (Figure 3P, 62%, n = 60). These embryos were much more lightly pigmented, suggesting that anterior neural crest formation was also affected (45%, n = 60), which might be a consequence of impaired anterior neural plate formation during gastrulation. Thus Shisa plays an important role in the anterior neuroectoderm formation. Consistently, *shisa*-MO injection into the animal side of blastomeres at the 4-cell stage resulted in similar head defects (Figure 3Q, 60%, n = 80), while embryos that received *shisa*-MO injections into the vegetal side were normal (Figure 3R, 80%, n = 40).

Shisa Inhibits Wnt Signaling in Responding Cells

To determine the molecular mechanism by which Shisa inhibits Wnt signaling, we examined Shisa function in HEK 293T cells. Expression of *X*Wnt8, *X*Frizzled 8 (Fz8), and human Lrp6 in HEK 293T cells activated luciferase expression driven by the reporter gene TOPFLASH, which contains multiple TCF/LEF binding sites (Korinek et al., 1997). Coexpression of Shisa inhibited the luciferase activity induced by Wnt8, Fz8, and Lrp6 (Figure 4B,

(M–N′) Partially restored *otx2* expression in *shisa*-MO injected embryo at early neurula. *shisa*-MO was radially injected at 4-cell stage and *otx2* expression was analyzed at stage 11.5 (M′) and stage 15 (N′). (M) and (N) give the expression in control embryos.

(O) Wild-type embryo at tadpole stage.

(P) Embryo injected shisa-MO as in (B).

(Q) Animal radial injection of shisa-MO at 4-cell stage.

(R) Vegetal radial injection of shisa-MO.

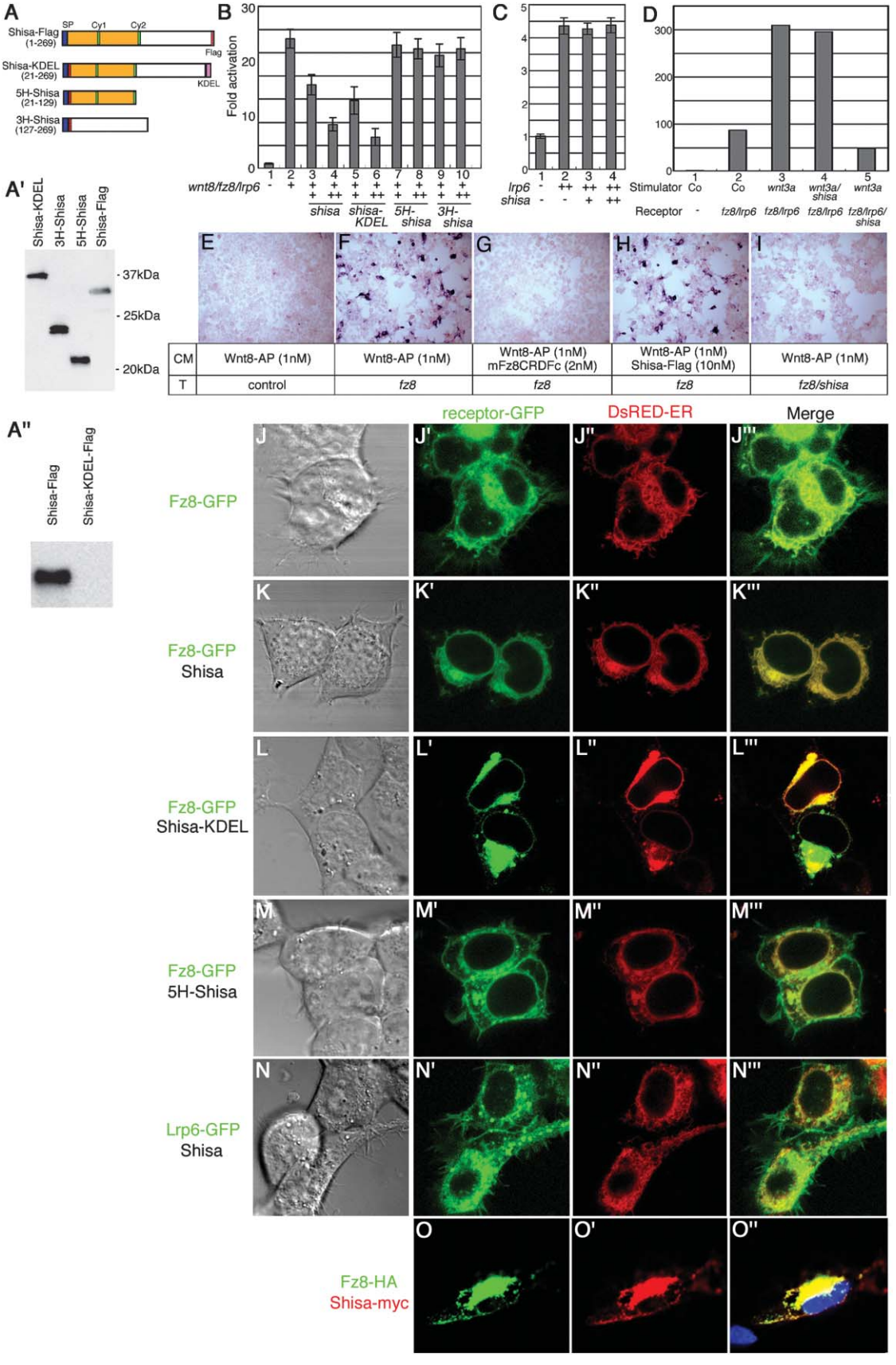
A
Shisa-Flag (1-269)
SP
Cy1
Cy2
Flag
Shisa-KDEL (21-269)
KDEL
5H-Shisa (21-129)
3H-Shisa (127-269)
B
Fold activation
wnt8/fz8/lrp6
shisa
shisa-KDEL
5H-shisa
3H-shisa
C
lrp6
shisa
D
Stimulator
Receptor
wnt3a
wnt3a/shisa
fz8/lrp6
fz8/lrp6/shisa
A'
Shisa-KDEL
3H-Shisa
5H-Shisa
Shisa-Flag
37kDa
25kDa
20kDa
E
F
G
H
I
CM
T
Wnt8-AP (1nM)
control
Wnt8-AP (1nM)
fz8
Wnt8-AP (1nM) mFz8CRDFc (2nM)
Wnt8-AP (1nM) Shisa-Flag (10nM)
Wnt8-AP (1nM)
fz8/shisa
A"
Shisa-Flag
Shisa-KDEL-Flag
receptor-GFP
DsRED-ER
Merge
Fz8-GFP
Fz8-GFP Shisa
Fz8-GFP Shisa-KDEL
Fz8-GFP 5H-Shisa
Lrp6-GFP Shisa
Fz8-HA Shisa-myc

lanes 3 and 4). Deletion of the either the amino half or the carboxy half of Shisa did not affect Wnt8-mediated TOPFLASH activity, indicating that both the domains are required to elicit its activity (Figures 4A, 4A′, and 4B, lanes 7–10). Expression of a large amount of Lrp6 alone induced the TOPFLASH activity at low level. Coexpression of Shisa did not inhibit Lrp6-mediated TOPFLASH activity (Figure 4C), suggesting that Shisa inhibits components other than Lrp6, and that Wnt8 and/or Fz8 may be involved in Shisa-mediated inhibition.

We next examined whether Shisa functions in signaling or receiving cells since Shisa has both a secreted and an ER-residing form (Figure 1). To address this question, we prepared two types of transfectant cells—stimulator and receptor cells—and carried out mixing experiments. The stimulator cells were transfected with either an expression vector for mouse Wnt3a or a mock control vector, and the receptor cells were transfected with vectors for Fz8, Lrp6, and the TOPFLASH reporter. When the Wnt3a-expressing stimulator cells were mixed with the receptor cells, TOPFLASH was strongly activated (4-fold, Figure 4D, lane 3). When Shisa was expressed in the stimulator cells, the TOPFLASH-mediated activity was not affected, suggesting that Shisa function is independent of the production and biological activity of the Wnt ligand. In contrast, when Shisa was expressed in the receptor cells, it suppressed the reporter activity to the basal level (Figure 4D, lane 5), indicating that Shisa functions autonomously in cells receiving Wnt signaling.

We further examined the effects of Shisa expression in the interaction between a Wnt ligand and Frizzled receptor (Figures 4E–4I). Wnt8-alkaline phosphatase (Wnt8-AP) fusion proteins efficiently bound to Fz8-expressing cells. This interaction was blocked by the addition of a soluble form of Fz8 (mFz8CRDFc) to the medium, but not by a secreted form of Shisa. In contrast, coexpressing Shisa with Fz8 significantly reduced Wnt8-AP binding (Figure 4I), further confirming that Shisa functions in cells receiving Wnt signaling.

Shisa Elicits Retention of Fz in the ER and Inhibits Its Expression on the Cell Surface

We next examined whether Shisa suppresses the cell surface expression of Fz. When GFP-tagged Fz8 was expressed in HEK 293T cells, Fz8-GFP was detected in both the cell surface and the ER, where DsRed-ER (Figures 4J–4J‴) and calreticulin (data not shown) were detected. In cells expressing both Fz8 and Shisa, Fz8 was accumulated in the ER (Figures 4K–4K‴). Furthermore, Fz8 and Shisa were colocalized (Figures 4O–4O″), indicating that the expression of Shisa induces retention of Fz8 in the ER and inhibits trafficking of Fz to the cell surface. Similarly, Shisa also promoted the retention of Fz7 in the ER (data not shown). Shisa expression did not affect the localization of Lrp6 (Figures 4N–4N‴). To confirm the function of Shisa in the ER, we constructed a Shisa protein tagged with the ER-retention signal KDEL (Shisa-KDEL) since Shisa has no ER retention signal. The KDEL signal effectively suppressed secretion of Shisa in the culture medium (Figure 4A″). Expression of Shisa-KDEL inhibited the Wnt8-dependent TOPFLASH activation and induced the retention of Fz8 in the ER, as Shisa did (Figures 4B and 4L–4L‴). Deletion mutants of the amino half or the carboxy half of Shisa failed to retain Fz8 in the ER (Figures 4M–4M‴ for 5H-Shisa, data not shown for 3H-Shisa). Moreover, the conditioned medium of the Shisa-expressing cells did not affect the localization of Fz8 (Supplemental Figure S2 on the *Cell* website). These results strongly suggest that Shisa functions in the ER to control the cellular transportation of Fz and thereby to inhibit Wnt signaling.

Figure 4. Shisa Cell-Autonomously Inhibits Wnt Signaling by Retaining Fz within the ER

(A) Schematic drawing of Shisa, fused with the ER retention KDEL signal, and deletion constructs employed. Shisa-KDEL, 5H-Shisa, and 3H-Shisa were generated by fusing a cassette containing a heterologous signal peptide followed by a Flag sequence to shisa cDNA fragments. Numbers in parentheses indicate corresponding Shisa amino acid residues.

(A′) Western blotting with α-Flag mAb shows equivalent protein productions of each construct. Cells were transfected with each construct (100 ng) in 12-well plate.

(A″) KDEL signal suppressed secretion of Shisa. Cells were transfected as in (A′).

(B) Shisa and Shisa-KDEL, but not 5H- and 3H-shisa, inhibited TOPFLASH reporter activation induced by XWnt8-Fz8-Lrp6 expression. Luciferase activities are indicated as fold activation/repression compared with the activity obtained from cells transfected with empty-vector and reporter (lane 1). Each experiment was carried out at least in triplicate, and error bars represent the standard deviation. Transfection was carried out in a 96-well plate with DNAs (per well): TOPFLASH reporter, 10 ng; *nlacZ*, 1 ng; *Xwnt8*, 5 ng; *fz8*, 1 ng; *lrp6*, 1 ng; *shisa, shisa-KDEL, 5H-shisa*, and *3H-shisa*, 5 ng (+) or 25 ng (++).

(C) Shisa failed to inhibit the signaling induced by a high dose of Lrp6 alone. DNA used: *lrp6*, 20 ng; *shisa* 5 ng for lane 3; and 25 ng for lane 4.

(D) Shisa cell-autonomously inhibited Wnt signaling in the cells receiving the signal. Stimulator and receptor cells were transfected separately and mixed in the combination presented at the bottom of the figure. Co: Cells transfected with the empty-vector alone. DNA used: *mwnt3a*, 500 ng; *fz8*, 8 ng; *lrp6*, 8 ng; TOPFLASH reporter, 80 ng; *nlacZ*, 8 ng; *shisa*, 200 ng.

(E–I) Shisa suppressed Wnt8-AP and Fz8 interaction. Live cells were stained with 1 nM of Wnt8-AP. Cells in an 8-well chamber slide were transiently transfected with DNAs: *fz8*, 2 ng; *shisa*, 50 ng. CM, condition media used. T, construct used for transfection.

(J–O″) Confocal immunofluorescent images of HEK 293T cells. Phase contrast images were (J), (K), (L), (M), and (N). ER was marked by DsRedER in (J″), (K″), (L″), (M″), and (N″).

(J–J‴) Transfected with *fz8*-GFP (green) (cell surface expression of Fz, n = 100, 98%).

(K–K‴) Transfected with *fz8*-GFP and *shisa* (ER retention of Fz, n = 100, 90%).

(L–L‴) Transfected with *fz8*-GFP and *shisa*-KDEL (ER retention of Fz, n = 100, 84%).

(M–M‴) Transfected with *fz8*-GFP and 5H-*shisa* (cell surface expression of Fz, n = 100, 92%).

(N–N‴) Transfected with *lrp6*-GFP and *shisa* (cell surface expression of Lrp6, n = 100, 86%).

(O–O″) Transfected with *fz8*-HA and *shisa*-myc (colocalization, n = 100, 84%).

Cells were transfected in an 8-well glass chamber with DNAs: *fz8*-GFP, 2 ng; *Lrp6*-GFP, 2 ng; *fz8*-HA, 2 ng; *shisa*, 50 ng; *shisa*-KDEL, 50 ng; 5H-*shisa*, 50 ng; *shisa*-Myc, 50 ng; pDsRed-ER, 10 ng.

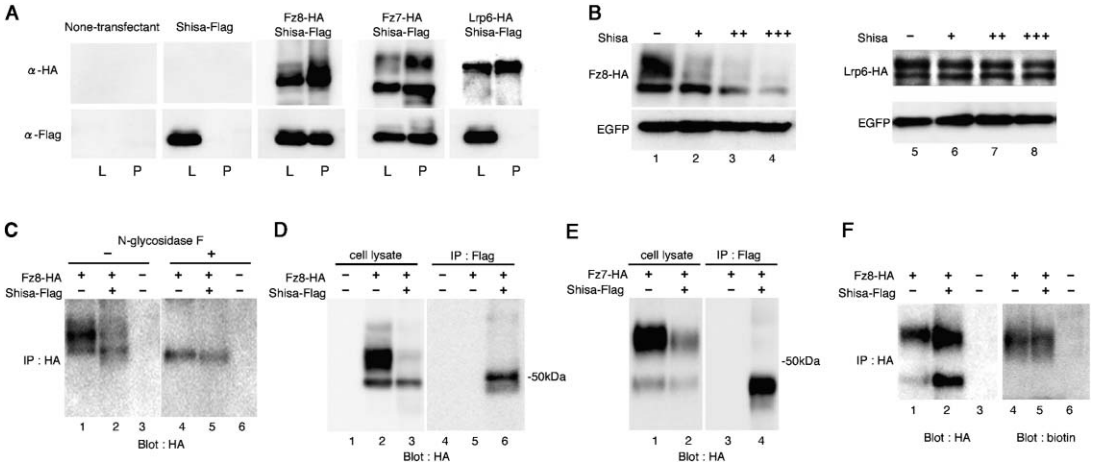

Figure 5. Effect of Shisa on Biochemical Property of Fz

(A) Shisa physically interacted with Fz8 and Fz7. Lysate of cells expressing proteins (indicated at top) was immunoprecipitated with rabbit α-HA Ab and blotted with rat α-HA mAb or mouse α-Flag mAb. Lysate (L) and the precipitate (P) were assayed for the presence of Shisa (bottom) or the receptor (top). Lysate and precipitate of none-transfectant served as a control for immunoprecipitation and Western blotting.

(B) Shisa reduced the molecular weight and protein expression of Fz8 but not that of Lrp6. Transfection was carried out in a 12-well plate with DNAs: *fz8*-HA, 20 ng; *lrp6*-HA, 20 ng; *EGFP*, 100 ng; *shisa*, 100 ng (lanes 2 and 6), 200 ng (lanes 3 and 7), or 400 ng (lanes 4 and 8).

(C) Molecular weight change of Fz8 was caused by impaired glycosylation. Immunoprecipitated Fz8-HA with rabbit α-HA Ab was treated with N-glycosidase F (lanes 4 and 5) and blotted with rat α-HA mAb.

(D and E) Fz8 (D) and Fz7 (E) coimmunoprecipitated with Shisa were low molecular weight forms only. Lysate of cells expressing indicated proteins at top was immunoprecipitated with α-FLAG mAb and blotted with rabbit α-HA Ab.

(F) Biotinylation of cells expressing Fz8-HA with or without Shisa. The levels of biotinylated Fz8 in the immunoprecipitate by rabbit α-HA Ab were determined by probing the blots with avidin-peroxidase conjugate (right).

Except (B), cells were transfected in a 6-well plate with DNAs: *fz8*-HA, 100 ng; *fz7*-HA, 100 ng; *lrp6*-HA, 100 ng; *shisa*-Flag, 200 ng.

Shisa Interacts with an Immature Form of Fz and Blocks Its Protein Maturation

We next examined the physical interaction between the Shisa and Fz proteins. Fz8-HA, Fz7-HA, or Lrp6-HA was coexpressed with Shisa-Flag in HEK 293T cells and then subjected to immunoprecipitation with a receptor, using α-HA Ab. Shisa was coimmunoprecipitated with Fz8 and Fz7, but not with Lrp6 (Figure 5A), indicating that Shisa physically interacts with Fz. Two species of Fz8-HA proteins of different molecular weights were detected by SDS-PAGE in the transfected HEK 293T cells (Figure 5B, lane 1). Expression of Shisa preferentially reduced the larger Fz8 protein; increasing amounts of Shisa reduced the smaller Fz8 proteins as well (Figure 5B, lanes 1–4) but did not affect the expression of Lrp6 protein (Figure 5B, lanes 5–8). The smaller Fz8 was not a degradation product of the mature (larger) Fz8 since treatment with N-glycosidase F reduced the molecular weight of both the larger and smaller Fz8 to the same level (Figure 5C). Therefore, the smaller Fz8 is thought to be an immature glycosylated form of Fz8. Shisa specifically interacted with the smaller, immature forms of Fz8 and Fz7 (Figures 5D and 5E). We further examined surface expression of the larger and smaller Fz proteins by the biotinylation of cell surface proteins. Only the larger form of Fz8 protein was labeled with biotin, indicating that the larger Fz8 protein is a mature form expressed on the cell surface (Figure 5F). Taken together with the immunofluorescence data (Figure 4), we conclude that Shisa interacts with the immature forms of Fz proteins, induces retention in the ER, and suppresses the protein maturation of Fz.

Shisa Protects Anterior Neuroectoderm from Wnt Signaling

We further examined whether Shisa is involved in Fz localization in *Xenopus* embryo. When Fz8-GFP fusion protein was expressed in *Xenopus* animal cap explants (ACs), it was detected on the cell surface (Figure 6A). Coexpression of Shisa inhibited the surface expression of Fz8-GFP and accumulated Fz8-GFP in the cytoplasm (Figure 6B). The cytoplasmic Fz8-GFP was colocalized with DsRed-ER (Figures 6D–6F), indicating that the expression of Shisa promotes the retention of Fz8 in the ER in the *Xenopus* embryos as well. Shisa expression reduced the larger form of Fz8 in the ACs but did not affect the protein expression of Lrp6 (Figure 6C).

Animal cap cells weakly express *shisa* endogenously, and Chordin (Chd), which induces anterior neuroectoderm, enhances *shisa* expression (Figure 6K, lanes 2 and 3). Thus Chd-expressing animal cap explants may serve as a valuable system for assaying the functions of endogenous Shisa. In these explants, Fz8-GFP localized both in the cytoplasm and on the cell surface (Figure 6G). Injection of *shisa*-MO markedly reduced the cytoplasmic accumulation and enhanced the cell-surface expression of Fz8-GFP in the explants (Figure 6H), suggesting that endogenously Shisa is involved in the regulation of cell-surface expression of Fz in the neuralized ectoderm.

We also confirmed that the loss of endogenous Shisa

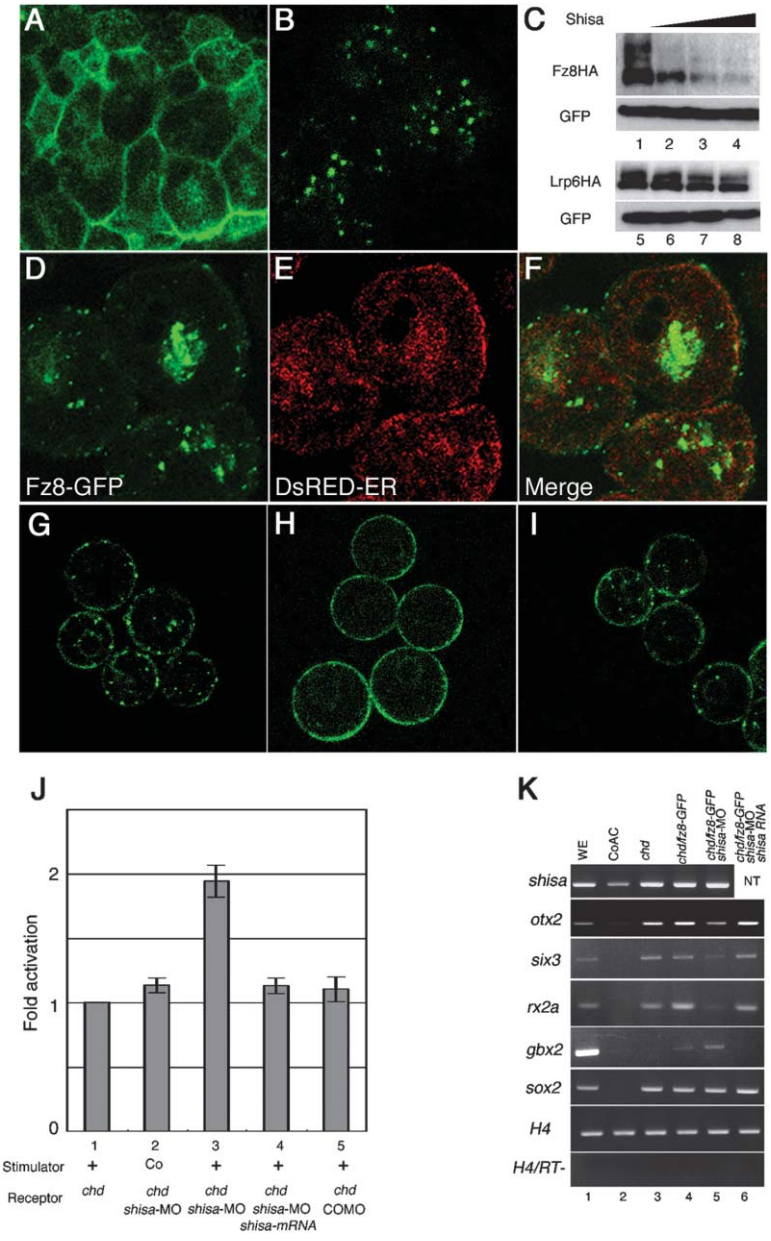

Figure 6. Role of Shisa in Fz Receptor Presentation and Wnt Signaling Attenuation

(A, B, and D–I) Confocal images of live ACs. (A and B) Radial injection of *fz8-GFP* RNA (10 pg) alone (A) or together with *shisa* RNA (20 pg) (B) into the each blastomere at 4-cell stage.

(C) Radial injection of *fz8*-HA RNA or *lrp6*-HA RNA (20 pg) together with *GFP* RNA (50 pg). Increased amount of *shisa* RNA (lanes 2 and 6, 5 pg; lanes 3 and 7, 10 pg; lanes 4 and 8, 20 pg) reduced molecular weight and expression of Fz protein. ACs of late blastula were lysed and blotted with rabbit α-HA Ab or α-GFP mAb.

(D–F) Coinjection of *fz8*-GFP and *shisa* RNA together with *DsRed-ER* RNA (50 pg). Shisa-mediated Fz8 accumulation was colocalized with DsRed-ER.

(G–I) Radial injection of *fz8*-GFP and *chd* RNA (25 pg) (G) or together with 10 ng of *shisa*-MO (H). Knockdown of Shisa reduced accumulation and promoted cell surface expression of Fz8-GFP. Additional injection of *shisa* RNA (10 pg) restored the accumulation of Fz8-GFP in the cytoplasm (I).

(J) Cell mixing assay of AC blastomere. Stimulator and receptor cells were prepared from the five ACs radially injected with *wnt3a* RNA (30 pg per blastomere) and with DNA or RNA listed at the bottom of figure together with TOPFLASH reporter (25 pg) and *lacZ* RNA (5 pg), respectively. Theses cells were combined at stage 11.5 and further incubated for next 3 hr. Co: ACs from uninjected embryos.

(K) Fz8-GFP and *shisa*-MO synergistically promoted posterior and suppressed anterior neural fate in *chd*-injected ACs. ACs injected with MO and RNA indicated at top of figure were analyzed for expressions of regional neuroectodermal markers at the stage 13.

function indeed enhances the response to Wnt-ligand stimulation; this was conducted by a mixing assay using ACs that received injections of *wnt3a* RNA (stimulator) or TOPFLASH reporter plasmid (receptor, Figure 6J). In this assay, the endogenous Shisa was enhanced in the receptor cells by *chordin*, as noted above. Coinjection of *shisa*-MO in the receptor cells increased Wnt3a-dependent TOPFLASH activity (Figure 6J, lane 3), indicating that the inhibition of endogenous Shisa function elicits sensitization to Wnt signaling. Consistent with this, coinjection of *shisa*-MO together with Fz8-GFP reduced the expression of anterior neuroectoderm markers (*otx2, six3*, and *rx2a*) but increased the expression of the hindbrain marker *gbx2* (Figure 6K, lane 5). All of these data strongly suggest that endogenous Shisa functions to protect anterior neuroectoderm from Wnt signaling by regulating the surface expression of Fz.

Shisa Affects the Maturation of FGFR

We next investigated the role of Shisa in FGF signaling. In transfected HEK 293T cells, Shisa interacted with FGFR but not with the Activin receptors, ActRI and ActRII (Figure 7A). Similarly to Fz, FGFR displayed two bands in SDS-PAGE in the transfected cells. Shisa expression reduced the larger (mature) form of FGFR (Figure 7B). Shisa interacted only with the smaller (immature) form of FGFR (Figure 7B) and induced retention of FGFR in the ER (Figures 7C–7C‴ and 7D–7D‴). Stimulation with FGF induced tyrosine phosphorylation of the mature form of FGFR in the cells expressing only FGFR (Figure

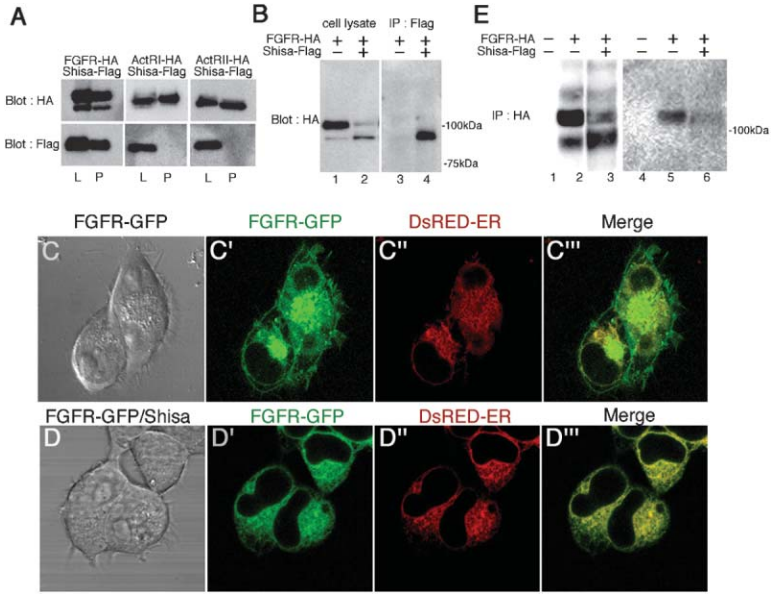

Figure 7. Shisa Inhibits Protein Maturation of FGFR

(A) Shisa physically interacted with FGFR but not with ActRI or ActRII. Immunoprecipitation analysis was carried out as described in Figure 5. Cells were transfected in a 6-well plate with DNAs: *fgfr*-HA, 300 ng; *ActRI*-HA, 100 ng; *ActRII*-HA, 10 ng; *shisa*-Flag, 200 ng.

(B) Coimmunoprecipitated FGFR-HA with Shisa was low molecular weight form only.

(C–D‴) Confocal images of live HEK 293T cells show the cellular localization of FGFR-GFP (green) and DsRed-ER (Red). Cells were transfected in an 8-chamber slide with DNAs: *fgfr*-GFP, 20 ng; *shisa*, 50 ng; pDsRedER, 10 ng. (C–C‴) Transfectant of *fgfr*-GFP (cell surface expression of FGFR, n = 100, 95%). (D–D‴) Transfected *fgfr*-GFP with *shisa* (ER retention of FGFR, n = 100, 92%).

(E) Shisa inhibited tyrosine-phosphorylation of FGFR. After stimulation with FGF2, lysate of cells expressing DNAs indicated at top was immunoprecipitated with rabbit α-HA Ab and was blotted with rat α-HA mAb (left) or mouse α-phosphotyrosine mAb (right).

7E, lane 5), but not in cells expressing both FGFR and Shisa (Figure 7E, lane 6). These data suggest that, as observed for Fz, Shisa interacts with the immature form of FGFR, elicits its retention in the ER, and thereby inhibits FGF signaling.

Discussion

Shisa Is a Novel Molecule in Head Formation

We report here the isolation of a novel factor, Shisa, which cell-autonomously attenuates the caudalizing signals, Wnt and FGF, in the future head territory of *Xenopus* gastrulae. Many studies have dealt with the essential roles of BMP, Wnt, and Nodal inhibitors secreted from the Spemann organizer in the induction of anterior neuroectoderm during gastrulation. However, few studies have considered the mechanisms that function in the ectoderm. In zebrafish, *tcf3/headless* and *axin/masterblind* inhibit the canonical Wnt signaling pathway in the anterior ectoderm and are required for head formation (Kim et al., 2000; Heisenberg et al., 2001; Dorsky et al., 2003). These reports suggest that, in addition to the inductive (non-cell-autonomous) factors derived from organizer tissues, the anterior ectoderm may protect itself from caudalizing signals by cell-autonomous mechanisms. Our results demonstrate that Shisa contributes to such an activity in the head ectoderm but functions by a novel molecular mechanism.

Specificity of Shisa

We found that Shisa functions as an inhibitor for the caudalizing signals Wnt and FGF but does not inhibit BMP and Actvin/Nodal signaling in head formation process during gastrulation (Figure 2). However, our preliminary analysis showed that, in HEK 293T cells, Shisa also retained Smoothened in the ER. Therefore it might be possible that Shisa exhibits its activity on a subset of seven-pass transmembrane proteins. Future phenotypic analyses of the *shisa*-MO-injected embryos will be required to reveal the functions of Shisa in signaling of Hedgehog and G protein-coupled receptors.

Role and Regulation of Shisa in Head Formation

In order produce Shisa activity specifically in the prospective head region, the expression of *shisa* needs to be under strict control. We observed a coordinated expression of *shisa* in the anterior endomesoderm (Spemann organizer) and the prospective head ectoderm (Figure 1) at times and sites appropriate to the head formation process. The situation is reminiscent of *otx2* expression in *Xenopus* in the anterior endomesoderm and head ectoderm (Blitz and Cho, 1995; Pannese et al., 1995).

In loss-of-function analysis by *shisa*-MO injection, we observed a predominant defect in the formation of anterior neuroectoderm (Figure 3), but no apparent abnormalities in the anterior endomesoderm or prechordal plate. In *shisa* morphant embryos, we have not observed a cyclopic phenotype, which is an indication of impaired prechordal plate formation (Figures 3N–3Q). Consistent with this, *shisa*-MO preferentially reduced ectodermal but not endomesodermal *otx2* expression (Figure 3C). Targeting *shisa*-MO to animal blastomeres gave similar head defects whereas to vegetal blastomeres had no effect for head formation (Figure 3). Inhibition of Wnt signaling is known to be involved in the development of the prechordal plate in both gain- and loss-of-function analyses (Glinka et al., 1998; Kazanskaya et al., 2000). Thus, Shisa functions redundantly with other Wnt inhibitors, such as Dkk-1, Frzb-1, and Cerberus, expressed in the anterior endomesoderm. However, since, uniquely among the cell surface regulators of Wnt signaling, *shisa* is expressed in the entire future head ectoderm, the ectodermal function of Shisa might be more important than its function in endomesoderm for proper head formation.

Shisa is the first molecule shown to inhibit both Wnt and FGF signaling. In *Xenopus* and zebrafish, gain- and

loss-of-function of FGF signaling leads to caudalization and rostralization of neuroectoderm, suggesting that the inhibition of FGF signaling could be involved in head formation as is the inhibition of Wnt signaling. It has not been clear whether there is a regulatory mechanism that controls FGF signaling in the head ectoderm of gastrulae. The present data show that Shisa cell-autonomously inhibits FGF signaling in both *Xenopus* and a human cell line (Figures 2 and 7), strongly implicating Shisa in the suppression of FGF signaling during head formation within the prospective head ectoderm. However, in *Xenopus* and zebrafish, it has been reported that Wnt and FGF signals caudalize the anterior neuroectoderm in a combinatorial manner (McGrew et al., 1997; Domingos et al., 2001; Kudoh et al., 2002), making it difficult to evaluate which function of Shisa is more strongly involved in head formation, or whether the involvement is equal. In the future, mutational analysis of Shisa may enable the separation of these two inhibitory activities and help to clarify their individual roles in vivo.

Molecular Mechanism of Shisa Action

Shisa is secreted in HEK 293T cells when overexpressed (Figure 1B), suggesting a non-cell-autonomous action. However, our data indicate that Shisa functions cell-autonomously in the ER, which suggests that a population of Shisa proteins reside in ER. Shisa has no ER retention signal, but it does have a hydrophobic region at the amino-terminal to the Cy2 region (Supplemental Figure S1), raising the possibility that Shisa is a transmembrane protein under physiological conditions. Our overexpression studies in HEK293T cells do not support this possibility; immunostaining with specific anti-Shisa antibodies will be required to reveal the localization of endogenous Shisa proteins.

Shisa interacted with immature forms of Fz and FGFR, elicited their retention within the ER, suppressed further processing of N-linked glycosylation, and reduced protein expression (Figures 5, 6, and 7). Cells expressing both Shisa and the receptors were not able to express the functional receptor protein properly on the cell surface and were incapable of responding to Wnt and FGF ligands (Figures 4 and 7). Overall the results support our claim that Shisa is an ER protein and a regulator of protein maturation of particular signaling receptor. In the ER, receptor proteins are generated and subjected to early processing of N-linked sugar modification in a process coupled to protein folding. If these proteins are misfolded, the QC system retains them in the ER, induces their aggregation by interchain disulfide bonds, and disposes of them by several protein degradation pathways outside of the ER (Tsai et al., 2002; Ellgaard and Helenius, 2003; Trombetta and Parodi, 2003). The impaired protein properties of Fz and FGFR resulting from Shisa function closely fit the criteria for misfolded proteins, suggesting that Shisa induces misfolding in Frizzled and FGFR, which leads to their degradation possibly through the QC system. Future structural analysis of Frizzled and FGFR associated with Shisa and identification of a molecule that provides a direct link between Shisa and QC system will clarify the more precise mechanism by which Shisa suppresses the post-translational maturation of these receptor proteins.

In summary, Shisa is a novel molecule that controls head formation through the inhibition of maturation in receptors of the caudalizing factors, Wnt and FGF. These findings may also shed light on the mechanism by which the ER regulates signal transduction machinery during development.

Experimental Procedures

Construction of Subtracted Anterior-Dorsal Endomesoderm (ADE) cDNA Library and Screening

Xenopus mid-gastrula (Stage 11.5) ADEs were isolated manually with a hair loop. Following the isolation of the upper dorsal lip region, the ectoderm and posterior half of the tissue block were removed and poly A^+ RNA was extracted by a standard procedure. cDNAs derived from 5 μg poly A^+ RNA were ligated with the ZAPII phagemid vector (Stratagene). The average length of the insert was 2.5 kb. For further enrichment of the genes specifically expressed in the ADE, the library was converted to a single-strand DNA by helper phage infection and subtracted using biotinylated early neurula trunk-tail and early gastrula ventral marginal zone mRNAs. By this subtraction, six hundred clones were obtained from 10^6 original clones. Those clones were sequenced and their expression patterns analyzed by whole-mount in situ hybridization as described elsewhere (Sive et al., 2000).

Embryonic Manipulations

Frog care, fertilization, and embryonic culture were carried out as described elsewhere (Sive et al., 2000). Animal cap explants (ACs) were excised at stage 9 and cultured in 0.5$\times$ MMR. For stimulation with Activin or FGF2, explants were cultured 3 hr in 1$\times$ LCMR with 0.1% bovine serum albumin (BSA) containing 5 ng/ml human recombinant Activin (R&D Systems) or 500 ng/ml human recombinant FGF2 (R&D Systems), respectively. Some explants were cultured further in 0.5$\times$ MMR up to sibling embryos reaching stage 20. β-galactosidase activity of nuclear lacZ RNA was visualized by 6-chloro-3-indolyl-β-galactoside (Red Gal, Research Organics). ACs were lysed by NP-40 lysis buffer: TBS-EDTA (50 mM Tris pH7.5, 150 mM NaCl, 5 mM EDTA) containing 0.5% NP-40 and protease inhibitor cocktail (Roche). Western blots were performed with Abs for activated and total ERK (Cell Signaling), α-Actin mAb (Sigma), and α-(α)-tubulin mAb (Sigma). To analyze cellular localization of Fz8-GFP in living blastomeres, ACs were dissected at the late blastula stage and cultured in the fibronectin (20 μg/ml, Sigma) coated cover glass chamber with the Ca/Mg-free MBS. After removing the pigmented surface ectoderm, cells were further incubated by the stage indicated.

Expression Constructs, Synthesis mRNAs, and Morpholino Oligomers

The *shisa* open reading frame was subcloned into pCS2 (*shisa*/pCS2). Myc-, Flag-, and HA-tag sequences were added to the C-terminals of the coding sequences by PCR to generate *shisa*-Myc/pCS2, *shisa*-Flag/pCS2, *fz8*-HA/pCS2, *fz7*-HA/pCS2, *lrp6*-HA/pCS2, *fgfr*-HA/pCS2, *ActRI*-HA/pCS2, *ActRII*-HA/pCS2. GFP fusion constructs were generated by fusing a cassette containing a GFP sequence to the cording sequence of receptors. To mark ER in living cells, pDsRedN2-ER (Clontech) was used. For synthesis RNAs, *shisa*, *shisa*-Flag, *Xwnt8*, *Xdsh*, *dngsk3*, β-*catenin*, *Xefgf*, *dnXfgfr*, *ras-V12*, *dkk-1*, *fzb-1*, and *nlacZ* constructs were linearized by NotI and *dnBMPR* by EcoRI and transcribed with SP6 RNA polymerase (Ambion). GFP RNA was synthesized from pβ*GFP*/RN3P vector linearized by SfiI with T3 RNA polymerase (Ambion). Morpholino antisense oligomers were obtained from Gene Tools. *shisa*-MO had the sequence 5′-CATGATAGGGAAACGTTATAATGAG-3′ and the standard control morpholino 5′-CCTCTTACCTCAGTTACAATTTATA-3′ used as a negative control.

Northern Blot and RT-PCR

Northern blot was carried out by a standard protocol using ^{32}P-labeled full-length *shisa* cDNA as a probe. The probed membrane was detected with FLA-3000G Bio-image-analyzer (Fuji film). RT

reactions were carried out with MLTV (Invitrogen) using 1 μg of total RNA in 50 μl total reaction volume. Two microliters of the RT-product was used for total 20 μl of PCR reaction. The PCR condition was denaturation, 30 s, 95°C; annealing, 30 s, 55°C; elongation, 30 s, 72°C. Gene-specific primers and cycles used were listed in Supplemental Table S1. PCR products were analyzed on 2% agarose gels with ethidium bromide staining.

Luciferase Assay

HEK 293T cells were transfected in a 96-well plate with Lipofectamin Plus (Invitrogen). The TOPFLASH activity of each sample was normalized against cotransfected β-galactosidase activity. For the cell-mixing assay, stimulator and receptor cells were transfected separately in a 12-well plate. Following overnight culture, cells were trypsinized and stimulator cells were mixed with receptor cells at the ratio of 3:1. A total of 4×10^4 cells were reseeded into a new 48-well plate. Following 12 hr incubation, luciferase activity was analyzed.

Production of Fusion Protein and Wnt8AP Cell Binding Assay

Condition media containing Fz8CRD-Fc and Shisa-Flag were obtained from HEK 293T cells transiently transfected with *mfz8CRD-Fc*/pRK5 and *shisa*-Flag/pCS2, respectively, under a serum-free condition. Wnt8myc-AP was produced as described elsewhere (Hsieh et al., 1999). The concentration of Shisa-Flag was determined by Western blotting against quantified Shisa-Flag affinity purified with anti-Flag M2 affinity gel column (Sigma). For mFz8CRD-Fc and Wnt8myc-AP, quantified mFz8CRD-Fc and Wnt8myc-Fc purified with protein G gel column (Amersham) were used as a standard, respectively. Wnt8-AP cell binding assay was carried out as described elsewhere (Hsieh et al., 1999).

Immunofluorescent Staining

Cells were transfected on a poly-L-Lysine coated chamber-slide and incubated for 24 hr and stained with a standard protocol. Primary Abs: mouse α-Myc mAb (9E10, Covance), rat α-HA mAb (3F10, Roche), rabbit anti-calreticulin Ab (StressGen) were used in 1:500 dilution. Second Abs: Alexa Fluor (AF) 660-conjugated α-mouse IgG or α-rabbit IgG, and AF 488-conjugated α-rat IgG (Molecular Probes) were used in 1:200 dilution. For the staining of *Xenopus* embryos, whole embryos were fixed by 4% PFA for 1 hr and mounted in 20% fish gelatin (Sigma). Cryotissue sections were stained with α-Flag mAb (Sigma) in 1:500 dilution.

Coimmunoprecipitation, Cell Surface Biotin Labeling, FGFR Phosphorylation Assay, and N-Glycosidase F Treatment

HEK 293T cells were transfected in a 6-well plate and were lysed in 500 μl of TBS-EDTA containing 1% Triton X-100 and a protease inhibitor. After 30 min incubation on ice, uncleared lysate was centrifuged and the supernatant was taken as lysate. For coimmunoprecipitation, 400 μl lysate was pre-cleared once with protein G beads alone and immunoprecipitated with α-Flag M2 mAb or rabbit α-HA polyclonal Ab (Covance) for 2 hr at 4°C under constant rotation. The lysate and resuspended precipitate were separated by sodium dodecyl sulfate (SDS)-polyacrylamide gel electrophoresis, blotted onto immobilon-P PVDF membrane (Millipore) and probed with rat α-HA (3F10) mAb or α-Flag M2 mAb. Probed membranes were detected by ECL plus (Amersham) and analyzed by LAS-1000 mini lumino-image analyzer (Fuji film). Cell surface biotin labeling was carried out according to the manufacture's protocol in which cells were labeled with 0.5 mg/ml sulfo-NHS-biotin (Pierce) in ice-cold PBS. For FGFR phosphorylation assay, transfectants were stimulated with 100 μg/ml FGF2 (R&D system) for 10 min. Immunoprecipitated FGFR was blotted with mouse α-phosphotyrosine 4G10 mAb (Upstate). For digestion of N-glycan, immunoprecipitated Fz was treated with 1 mU of N-glycosidase F (Roche) for 12 hr at 30°C.

Acknowledgments

We thank Drs. E. Amaya, A.H. Brivanlou, E.M. De Robertis, J. Gurdon, X. He, J.C. Hsieh, D. Kimmelman, C. Kintner, P.S. Klein, K. Koebernick, D. Melton, R.T. Moon, C. Niehrs, E. Nishida, R. Nuse, R. Rupp, S. Sokol, H. Steinbeisser, N. Ueno, and D.G. Wilkinson for gifts of plasmids. We gratefully acknowledge Drs. I.B. Dawid, K. Hatta, D. Sipp, K. Furushima, and K. Furukawa for helpful discussion and critical comments on this manuscript. This work was supported by Grants-in-Aid for Scientific Research on Priority Areas from the Ministry of Education, Culture, Sports, Science and Technology of Japan.

Received: April 23, 2004
Revised: September 8, 2004
Accepted: November 23, 2004
Published: January 27, 2005

References

Amaya, E., Musci, T.J., and Kirschner, M.W. (1991). Expression of a dominant negative mutant of the FGF receptor disrupts mesoderm formation in Xenopus embryos. Cell *66*, 257–270.

Blitz, I.L., and Cho, K.W. (1995). Anterior neurectoderm is progressively induced during gastrulation: the role of the Xenopus homeobox gene orthodenticle. Development *121*, 993–1004.

Bouwmeester, T., Kim, S., Sasai, Y., Lu, B., and De Robertis, E.M. (1996). Cerberus is a head-inducing secreted factor expressed in the anterior endoderm of Spemann's organizer. Nature *382*, 595–601.

Brannon, M., Gomperts, M., Sumoy, L., Moon, R.T., and Kimelman, D. (1997). A beta-catenin/XTcf-3 complex binds to the siamois promoter to regulate dorsal axis specification in *Xenopus*. Genes Dev. *11*, 2359–2370.

Cadigan, K.M., and Nusse, R. (1997). Wnt signaling: a common theme in animal development. Genes Dev. *11*, 3286–3305.

Chen, X., Rubock, M.J., and Whitman, M. (1996). A transcriptional partner for MAD proteins in TGF-beta signalling. Nature *383*, 691–696.

Cornell, R.A., and Kimelman, D. (1994). Activin-mediated mesoderm induction requires FGF. Development *120*, 453–462.

Cox, W.G., and Hemmati-Brivanlou, A. (1995). Caudalization of neural fate by tissue recombination and bFGF. Development *121*, 4349–4358.

Culi, J., and Mann, R.S. (2003). Boca, an endoplasmic reticulum protein required for wingless signaling and trafficking of LDL receptor family members in Drosophila. Cell *112*, 343–354.

De Robertis, E.M., Larrain, J., Oelgeschlager, M., and Wessely, O. (2000). The establishment of Spemann's organizer and patterning of the vertebrate embryo. Nat. Rev. Genet. *1*, 171–181.

Domingos, P.M., Itasaki, N., Jones, C.M., Mercurio, S., Sargent, M.G., Smith, J.C., and Krumlauf, R. (2001). The Wnt/beta-catenin pathway posteriorizes neural tissue in Xenopus by an indirect mechanism requiring FGF signalling. Dev. Biol. *239*, 148–160.

Dorsky, R.I., Itoh, M., Moon, R.T., and Chitnis, A. (2003). Two tcf3 genes cooperate to pattern the zebrafish brain. Development *130*, 1937–1947.

Ellgaard, L., and Helenius, A. (2003). Quality control in the endoplasmic reticulum. Nat. Rev. Mol. Cell Biol. *4*, 181–191.

Fainsod, A., Deissler, K., Yelin, R., Marom, K., Epstein, M., Pillemer, G., Steinbeisser, H., and Blum, M. (1997). The dorsalizing and neural inducing gene follistatin is an antagonist of BMP-4. Mech. Dev. *63*, 39–50.

Glinka, A., Wu, W., Onichtchouk, D., Blumenstock, C., and Niehrs, C. (1997). Head induction by simultaneous repression of Bmp and Wnt signalling in Xenopus. Nature *389*, 517–519.

Glinka, A., Wu, W., Delius, H., Monaghan, A.P., Blumenstock, C., and Niehrs, C. (1998). Dickkopf-1 is a member of a new family of secreted proteins and functions in head induction. Nature *391*, 357–362.

Harland, R., and Gerhart, J. (1997). Formation and function of Spemann's organizer. Annu. Rev. Cell Dev. Biol. *13*, 611–667.

Heisenberg, C.P., Houart, C., Take-Uchi, M., Rauch, G.J., Young, N., Coutinho, P., Masai, I., Caneparo, L., Concha, M.L., Geisler, R., et al. (2001). A mutation in the Gsk3-binding domain of zebrafish

Masterblind/Axin1 leads to a fate transformation of telencephalon and eyes to diencephalon. Genes Dev. *15*, 1427–1434.

Hsieh, J.C., Rattner, A., Smallwood, P.M., and Nathans, J. (1999). Biochemical characterization of Wnt-frizzled interactions using a soluble, biologically active vertebrate Wnt protein. Proc. Natl. Acad. Sci. USA *96*, 3546–3551.

Hsieh, J.C., Lee, L., Zhang, L., Wefer, S., Brown, K., DeRossi, C., Wines, M.E., Rosenquist, T., and Holdener, B.C. (2003). Mesd encodes an LRP5/6 chaperone essential for specification of mouse embryonic polarity. Cell *112*, 355–367.

Hunter, T. (1998). The role of tyrosine phosphorylation in cell growth and disease. Harvey Lect. *94*, 81–119.

Kadowaki, T., Wilder, E., Klingensmith, J., Zachary, K., and Perrimon, N. (1996). The segment polarity gene porcupine encodes a putative multitransmembrane protein involved in Wingless processing. Genes Dev. *10*, 3116–3128.

Kazanskaya, O., Glinka, A., and Niehrs, C. (2000). The role of Xenopus dickkopf1 in prechordal plate specification and neural patterning. Development *127*, 4981–4992.

Kim, C.H., Oda, T., Itoh, M., Jiang, D., Artinger, K.B., Chandrasekharappa, S.C., Driever, W., and Chitnis, A.B. (2000). Repressor activity of Headless/Tcf3 is essential for vertebrate head formation. Nature *407*, 913–916.

Korinek, V., Barker, N., Morin, P.J., van Wichen, D., de Weger, R., Kinzler, K.W., Vogelstein, B., and Clevers, H. (1997). Constitutive transcriptional activation by a beta-catenin-Tcf complex in APC−/− colon carcinoma. Science *275*, 1784–1787.

Kudoh, T., Wilson, S.W., and Dawid, I.B. (2002). Distinct roles for Fgf, Wnt and retinoic acid in posteriorizing the neural ectoderm. Development *129*, 4335–4346.

LaBonne, C., and Whitman, M. (1994). Mesoderm induction by Activin requires FGF-mediated intracellular signals. Development *120*, 463–472.

Lamb, T.M., and Harland, R.M. (1995). Fibroblast growth factor is a direct neural inducer, which combined with noggin generates anterior-posterior neural pattern. Development *121*, 3627–3636.

Leyns, L., Bouwmeester, T., Kim, S.H., Piccolo, S., and De Robertis, E.M. (1997). Frzb-1 is a secreted antagonist of Wnt signaling expressed in the Spemann organizer. Cell *88*, 747–756.

McGrew, L.L., Hoppler, S., and Moon, R.T. (1997). Wnt and FGF pathways cooperatively pattern anteroposterior neural ectoderm in Xenopus. Mech. Dev. *69*, 105–114.

McKendry, R., Hsu, S.C., Harland, R.M., and Grosschedl, R. (1997). LEF-1/TCF proteins mediate wnt-inducible transcription from the Xenopus nodal-related 3 promoter. Dev. Biol. *192*, 420–431.

Meno, C., Saijoh, Y., Fujii, H., Ikeda, M., Yokoyama, T., Yokoyama, M., Toyoda, Y., and Hamada, H. (1996). Left-right asymmetric expression of the TGF beta-family member lefty in mouse embryos. Nature *381*, 151–155.

Monsoro-Burq, A.H., Fletcher, R.B., and Harland, R.M. (2003). Neural crest induction by paraxial mesoderm in Xenopus embryos requires FGF signals. Development *130*, 3111–3124.

Moon, R.T., Bowerman, B., Boutros, M., and Perrimon, N. (2002). The promise and perils of Wnt signaling through beta-catenin. Science *296*, 1644–1646.

Niehrs, C. (1999). Head in the WNT: the molecular nature of Spemann's head organizer. Trends Genet. *15*, 314–319.

Pannese, M., Polo, C., Andreazzoli, M., Vignali, R., Kablar, B., Barsacchi, G., and Boncinelli, E. (1995). The Xenopus homologue of Otx2 is a maternal homeobox gene that demarcates and specifies anterior body regions. Development *121*, 707–720.

Piccolo, S., Agius, E., Leyns, L., Bhattacharyya, S., Grunz, H., Bouwmeester, T., and De Robertis, E.M. (1999). The head inducer Cerberus is a multifunctional antagonist of Nodal, BMP and Wnt signals. Nature *397*, 707–710.

Pownall, M.E., Tucker, A.S., Slack, J.M., and Isaacs, H.V. (1996). eFGF, Xcad3 and Hox genes form a molecular pathway that establishes the anteroposterior axis in Xenopus. Development *122*, 3881–3892.

Sasai, Y., Lu, B., Steinbeisser, H., Geissert, D., Gont, L.K., and De Robertis, E.M. (1994). Xenopus chordin: a novel dorsalizing factor activated by organizer-specific homeobox genes. Cell *79*, 779–790.

Semenov, M.V., Tamai, K., Brott, B.K., Kuhl, M., Sokol, S., and He, X. (2001). Head inducer Dickkopf-1 is a ligand for Wnt coreceptor LRP6. Curr. Biol. *11*, 951–961.

Sive, H.L., Grainger, R.M., and Harland, R.M. (2000). Early Development of Xenopus laevis: A Laboratory Manual (Cold Spring Harbor, New York: Cold Spring Harbor laboratory Press).

Smith, W.C., and Harland, R.M. (1992). Expression cloning of noggin, a new dorsalizing factor localized to the Spemann organizer in Xenopus embryos. Cell *70*, 829–840.

Thisse, C., and Thisse, B. (1999). Antivin, a novel and divergent member of the TGFbeta superfamily, negatively regulates mesoderm induction. Development *126*, 229–240.

Thorpe, C.J., Schlesinger, A., Carter, J.C., and Bowerman, B. (1997). Wnt signaling polarizes an early C. elegans blastomere to distinguish endoderm from mesoderm. Cell *90*, 695–705.

Trombetta, E.S., and Parodi, A.J. (2003). Quality control and protein folding in the secretory pathway. Annu. Rev. Cell Dev. Biol. *19*, 649–676.

Tsai, B., Ye, Y., and Rapoport, T.A. (2002). Retro-translocation of proteins from the endoplasmic reticulum into the cytosol. Nat. Rev. Mol. Cell Biol. *3*, 246–255.

van den Heuvel, M., Harryman-Samos, C., Klingensmith, J., Perrimon, N., and Nusse, R. (1993). Mutations in the segment polarity genes wingless and porcupine impair secretion of the wingless protein. EMBO J. *12*, 5293–5302.

Wang, S., Krinks, M., Lin, K., Luyten, F.P., and Moos, M., Jr. (1997). Frzb, a secreted protein expressed in the Spemann organizer, binds and inhibits Wnt-8. Cell *88*, 757–766.

Accession Numbers

The open reading frame of *shisa* was deposited in GenBank with accession number AY579372.